

Structural effects on the phosphorylation of 3-substituted 1- β -D-ribofuranosyl-1,2,4-triazoles by human adenosine kinase

Sidath C. Kumarapperuma,^a Yanjie Sun,^b Marjan Jeselnik,^a Kiwon Chung,^a
William B. Parker,^b Colleen B. Jonsson^b and Jeffrey B. Arterburn^{a,*}

^aDepartment of Chemistry and Biochemistry, MSC 3C, New Mexico State University, Las Cruces, NM 88003, USA

^bSouthern Research Institute, 2000 Ninth Avenue South, Birmingham, AL 35205, USA

Received 3 February 2007; revised 6 March 2007; accepted 7 March 2007

Available online 12 March 2007

Abstract—The conversion of ribavirin to the monophosphate by adenosine kinase is the rate-limiting step in activation of this broad spectrum antiviral drug. Variation of the 3-substituents in a series of bioisosteric and homologated 1- β -D-ribofuranosyl-1,2,4-triazoles has marked effects on activity with the human adenosine kinase, and analysis of computational descriptors and binding models offers insight for the design of novel substrates.

© 2007 Elsevier Ltd. All rights reserved.

RNA viruses are significant pathogens that cause illnesses ranging from the common cold to epidemic scale diseases such as AIDS, hepatitis C, influenza, and emerging diseases caused by the agents Yellow fever virus, West Nile virus, Dengue virus, SARS CoV, and hantaviruses. Few antiviral drugs are available, and clinical treatment must confront the diversity and rapid evolution of resistant strains. The antiviral drug ribavirin (1- β -D-ribofuranosyl-1,2,4-triazole-3-carboxamide) **1** was first synthesized in 1972 and has shown broad spectrum antiviral activity against both RNA and DNA viruses.¹ Ribavirin has been used clinically in combination with interferon- α for treatment of hepatitis C virus (HCV) infection, respiratory syncytial virus (RSV), several viral hemorrhagic fever causing viruses, and recently for SARS CoV infections.^{2–5} Side effects, including hemolytic anemia,^{6,7} and viral resistance^{8,9} are major limitations.

The phosphorylation of ribavirin to the 5'-monophosphate by human adenosine kinase (hADK) is the rate-limiting step for activation to the physiologically relevant triphosphate.^{10–14} Several mechanisms for ribavirin's antiviral activity have been identified. It inhibits inosine 5'-monophosphate dehydrogenase and decreases intra-

cellular guanosine triphosphate (GTP) concentrations.¹⁵ This is the predominant mechanism for the antiviral activity of ribavirin against yellow fever, parainfluenza 3, and respiratory syncytial viruses.^{16–18} Other mechanisms of ribavirin's antiviral activity include: (1) inhibition of influenza virus RNA polymerase in vitro with ribavirin triphosphate (RTP),^{19,20} (2) inhibition of viral genome capping through interference with guanylttransferase or methyltransferase activity in Sindbis virus,^{21–23} and (3) modulation of host immune response in HCV infected patients.^{24,25} Recent interest has been focused on increased mutation rates in the viral genome that affect replication, transcription, and virion viability. This has been shown in the case of Hantaan virus, an Old World hantavirus that can produce a life-threatening hemorrhagic fever with renal syndrome.²⁶

There is great interest in the development of synthetic nucleoside analogs with modified hydrogen bonding, π -stacking, hydrophobic and steric features to exploit the decreased fidelity of viral replication and transcription.^{27,28} Considering the importance of hADK for metabolic activation of **1**, we were interested in evaluating structural effects within a closely related series of 3-substituted-1- β -D-ribofuranosyl-1,2,4-triazoles as part of our ongoing efforts to develop new antiviral drugs for RNA viruses.

We identified a series of triazole derivatives (**2–8**) with 3-substituents providing modified steric volume, lipophilicity,

Keywords: Ribavirin; Bioisostere; Adenosine kinase; Triazole; Antiviral.

* Corresponding author. Tel.: +1 505 646 2738; fax: +1 505 646 2649; e-mail: jarterbu@nmsu.edu

hydrogen-bonding capacity, and ionic charge. Compounds **2–4** possess isosteric substitutions for the 3-carboxamide of **1** including nitro, ketone, and carboxylate groups, respectively. Derivatives **5**, **7**, and **8** are homologs and constitutional isomers of **1** that incorporate an additional methylene group. The carbonyl oxygen of **1** was replaced with *N*-methyl in amidine derivative **6**.

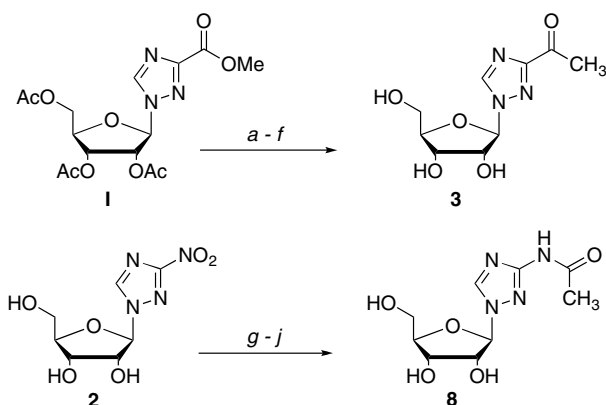
The nitro derivative **2** was prepared by direct fusion of 3-nitro-1,2,4-triazole with 1-*O*-acetyl-2,3,5-tri-*O*-benzoyl- β -D-ribofuranose.²⁹ The carboxylate **4** and *N*-methylcarboxamide **5** were obtained after deprotecting the commercially available methyl ester (**1**) followed by saponification or methylamine substitution, respectively.³⁰ The methyl ketone **3** and the acetamide **8** were synthesized as shown in Scheme 1.^{39,40} Introduction of *tert*-butyldimethylsilyl protecting groups followed by selective reduction of the methyl ester with diisobutylaluminum hydride provided the aldehyde, then addition of methylmagnesium bromide, oxidation with pyridinium chlorochromate, and deprotection gave the methyl ketone **3**. The acetamide **8** was synthesized from **2** by reduction of the nitro with hydrazine, followed by acetylation and ester hydrolysis. The *N*-methylamidine **6** and methyl imidate **7** were prepared from **1** following the literature route.³⁰ No hydrolysis of **6** or **7** was evident by ¹H NMR after two weeks in D₂O at 25 °C.

The hADK clone 20-1 was generously provided by Dr. Jozef Spychala (UNC Chapel Hill, Chapel Hill, NC) and hADK was prepared as described.³¹ Nucleosides were assayed as substrates for hADK, and reaction products were detected by HPLC. Assay conditions consisted of 50 mM Hepes (pH 6.0), 40 mM KCl, 1 mM MgCl₂, 1 mM ATP, 0.1% BSA, 10 μ M deoxycofomycin, 100 μ M of the test compound, and enzyme. Reactions were started by the addition of enzyme and incubated in a 37 °C water bath. Aliquots of 50 μ l were taken at 0-, 1-, 2-, and 4-h intervals, and reactions were

stopped by the addition of 50 μ l of 1 M perchloric acid. Samples were neutralized to pH 7, and precipitated salts were removed by centrifugation. Reactants and products were separated by HPLC using Bio Basic anion exchange column (Thermo Electron Corp., Bellefonte, PA) with a 40-min linear salt and pH gradient from 5 mM ammonium phosphate (pH 2.8) to 750 mM ammonium phosphate (pH 6). Peaks were detected as they eluted from the column by absorbance at their λ_{max} , typically 215 nm. All enzyme reactions were linear during the incubation period and substrate conversions were maintained at less than 10%.¹² The potential for inhibition of hADK activity was evaluated by monitoring the formation of ribavirin monophosphate in the presence of compounds **2–8**. The initial ribavirin concentration was 0.1 μ M, with individual compounds at 400 μ M.

The specific and relative activities for phosphorylation of **1–8** by hADK are shown in Table 1. Enzyme activity was only detected with four of the ribavirin analogs (**2**, **3**, **5**, and **6**). However, these analogs were less effective substrates than **1**. In addition, none of the ribavirin analogs (**2–8**) inhibited the phosphorylation of ribavirin by hADK (data not shown). Since a 4000-fold excess of compound did not inhibit the phosphorylation of ribavirin, these results indicated that the K_m of the analogs was much higher than the K_m for ribavirin. Because compound **2** had 18% of the activity of ribavirin but did not inhibit the phosphorylation of ribavirin, these results would suggest that **2** has a higher V_{max} than ribavirin.

Computational methods were used to characterize possible structural contributions to hADK activity within this series. Geometries were fully optimized in the gas phase at the B3LYP/6-31G** level of theory. In each case, computation identified the syn glycoside conformation of compounds **1–8** as the minimum energy conformers, in which N2 of the triazole base is oriented into the ribofuranose ring. These results are consistent with the reported conformational preference of **1** in solution as determined by NMR and circular dichroism.^{32,33} The validity of the calculated glycoside conformation of **2** was confirmed experimentally by observation of strong NOE correlation between H5-H1' in the NOESY spectrum.



Scheme 1. Synthesis of **3** and **8**. Reagents and conditions: (a) NaOCH₃, CH₃OH, rt, 2 h, 82%; (b) TBSCl, imidazole, DMAP, DMF, rt, 12 h, 84%; (c) DIBAL-H, CH₂Cl₂, -78 °C, 4 h, 78%; (d) CH₃MgCl, THF, 0 °C, 2 h, 87%; (e) PCC, CH₂Cl₂, mol sieves, rt, 4 h, 62%; (f) TBAF, THF, 0 °C, 2 h, 76%; (g) H₂NNH₂, H₂O, rt, 0.5 h, 89%; (h) Ac₂O, NEt₃, DMAP, CH₃CN, rt, 16 h, 55%; (i) CH₃COCl, NEt₃, CH₃CN, rt, 2 h, 59%; (j) NaOCH₃, CH₃OH, rt, 2 h, 64%.

Table 1. hADK activity of 3-substituted 1- β -D-ribofuranosyl-1,2,4-triazoles

Compound	Specific activity (nmol/mg h) ^a	% activity 1
1 (ribavirin)	203 (\pm 32)	100
2	36 (\pm 9)	18
3	20 (\pm 7)	10
4	<4	<2
5	19 (\pm 2)	9
6	11 (\pm 1)	5
7	<4	<2
8	<4	<2

^a Values are means of three experiments, standard deviation is given in parentheses.

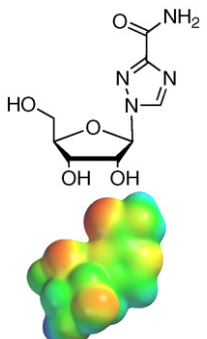
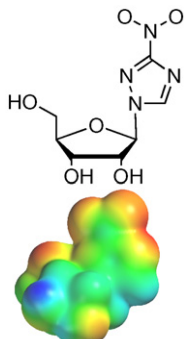
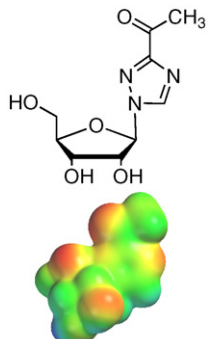
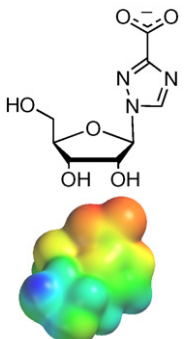
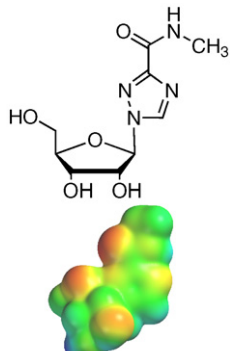
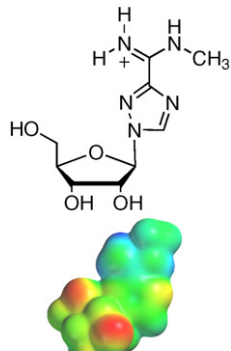
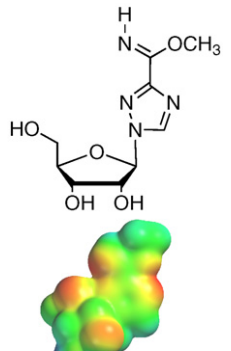
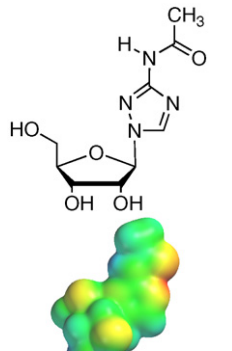
Computationally derived molecular descriptors have been shown to be useful for comparative evaluation of bioisosteres.³⁴ The electrostatic potential densities of **1–8** were mapped on the van der Waals surfaces in the space filling models using SPARTAN'06. The molecular electrostatic potential (MEP) mapped on the isodensity surface of the molecule provides a visual indicator for qualitative comparison of hydrogen bonding capacities, with a spectrum ranging from red representing high electron density to blue (Table 2).

Additional selected computational descriptors for **1–8** are listed in Table 3. Hydrophobic interactions can be approximated using complementary lipophilic profiles, the water accessible hydrophobic surface area of the molecule (CPK Area), and log *P* octanol/water partition coefficients (log *P*_{ow}). Comparison of long-range electrostatic interactions of neutral molecules can be approximated using the dipole moment/volume (μ/V). The descriptor for chemical hardness $\eta = (\text{LUMO} - \text{HOMO})/2$ provides an estimation of the aromaticity that relates to the propensity for π -stacking. The calculated η values for all of the compounds are similar (0.077–0.113 eV) and represent comparable π -stacking capacities across the series of substituted triazole bases.

The compounds evaluated fall within two general classes, isosteres possessing overall steric volume similar to **1** but altered functionality that affects H-bonding (**2–4**), and homologated analogs possessing increased steric profiles and altered hydrophobicity (**5–8**). The 3-nitro derivative **2** was the most active synthetic analog. This compound possesses a molecular electrostatic potential map that is similar to **1** (ribavirin), the smallest volume, highest lipophilicity and dipole moment/volume. The nitro group is isostructural to the carboxamide but typically exhibits weaker intermolecular H-bond accepting capabilities.³⁵ Nitrated base analogs have been extensively evaluated as potential universal bases where nitro-arenes typically form strong π - π stacking interactions through polarization of the (hetero) aryl ring.³⁶ The derivative β -ribofuranosyl-3-nitropyrrole was reported to undergo phosphorylation equivalent to ribavirin using hamster ADK.¹⁴ The ketone **3** is a structural mimic of **1** where replacement of the amine with methyl eliminates two H-bond donors. The activity of *N*-methyl derivative **5** was comparable with that of **3**, *N*-methylribamidine **6** was 20-fold less active than **1**, while **4**, **7**, and **8** were ineffective substrates.

Manual docking of the calculated minimum energy conformation of ribavirin into the hADK substrate binding

Table 2. Calculated molecular potential density maps^a

Compound	1	2	3	4
Isosteric series				
				
Compound	5	6	7	8
Homologated series				
				

^a Molecular electrostatic potentials were calculated at the B3LYP/6-31G** level and mapped on 0.002 au isodensity surface and are shown with identical chromatic scales (red is more negative, greater electron density; blue is more positive, less electron density). Spartan'06, Wavefunction, Inc. Irvine, CA.

Table 3. Calculated molecular properties

Compound	μ , D	CPK area A ²	CPK volume A ³	log <i>P</i>	μ/V , D/A ³	η , eV
1	4.5	238.11	210.7	−2.17	0.021	0.109
2	6	232.13	201.7	−0.58	0.026	0.087
3	5	245.53	219	−1.01	0.023	0.099
4	11.9	222.68	204.2	na	0.058	0.089
5	4.2	260.12	231.1	−1.935	0.018	0.108
6	(−)8.6	267.02	236.5	−2.07	0.036	0.077
7	1.9	259.86	230.9	−1.04	0.008	0.108
8	6.1	260.66	231.2	−1.68	0.026	0.113

site revealed the possibility of deeper penetration into the lipophilic pocket to enable π -stacking of the triazole with phenylalanine residue F170.³⁷ In this position, the carboxamide amine group of **1** mimics the critical N6-amine of adenosine that undergoes H-bonding to bound waters W416, and W415 associated with residues T173 and I39. The increased penetration of **1** into the substrate binding pocket would position the 5'-hydroxy group further from the bound ATP that is responsible for phosphorylation, resulting in reduced rates of phosphorylation relative to adenosine.

All of the 3-substituted 1,2,4-triazoles **2–8** were less efficient hADK substrates than **1**. Comparable π -stacking capacities are expected across the series based on the computed η -values. The nitro and methyl groups of **2** and **3** cannot interact as H-bond donors with W415 and W416, and the methyl of carboxamide **5** would effect these interactions, altering substrate orientation and enzyme structure compared with adenosine, resulting in decreased activity.^{37,38}

It is instructive to compare these results with other structurally modified nucleoside derivatives that are substrates for hADK (Fig. 1). The 7-deaza-purine, tubercidin, and related 7-carboxamido-purine derivative, sangivamycin, exhibit favorable electrostatic and π -stacking interactions and are excellent substrates for ADK.¹¹ In contrast, the 7-carbonitrile and 7-iodo analogs, toyocomycin, and tubercidin, are potent ADK

inhibitors due to displacement of W415 resulting in stronger hydrophobic interactions with I39.

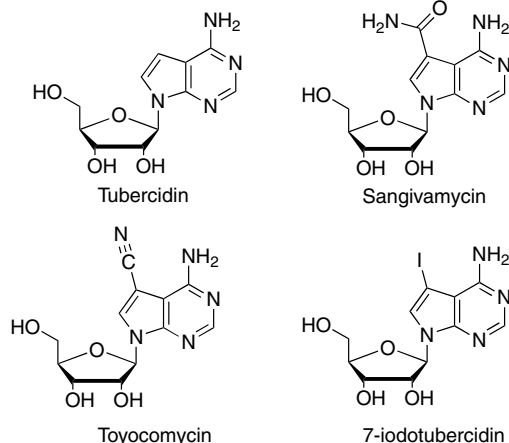
This study demonstrates that structural modifications significantly affect the hADK activity of 3-substituted 1- β -D-ribofuranosyl-1,2,4-triazoles. The ribavirin derivatives **4**, **7**, and **8** were ineffective substrates for hADK, and these results may correlate with the reported lack of antiviral activity against distinct viruses, although metabolism by other enzymatic pathways is not excluded.³⁰ The isosteric derivatives **2**, **3** and *N*-methyl homolog **5** were phosphorylated by hADK, and the antiviral activity of these compounds is currently under investigation. Consideration of computational descriptors and structural interactions provides insight substrate binding and activity into and provides direction for additional structural optimization for the development of antiviral nucleoside analogs with improved selectivity and reduced side effects.

Acknowledgments

This work was supported by Department of Defense USAMRC Grant No. W81XWH-04-C-0055 (C.J.), and NIH INBRE RR016480 (J.A.).

References and notes

- Sidwell, R. W.; Huffman, J. H.; Khare, G. P.; Allen, L. B.; Witkowski, J. T.; Robins, R. K. *Science* **1972**, *177*, 705.
- Gish, R. G. *J. Antimicrob. Chemother.* **2006**, *57*, 8.
- Chidgey, S. M.; Broadley, K. J. *J. Pharm. Pharmacol.* **2005**, *57*, 1371.
- Huggins, J. W. *Rev. Infect. Dis.* **1989**, *11*, S750.
- Booth, C. M.; Matukas, L. M.; Tomlinson, G. A.; Rachlis, A. R.; Rose, D. B.; Dwosh, H. A.; Walmsley, S. L.; Mazzulli, T.; Avendano, M.; Derkach, P.; Ephtimios, I. E.; Kitai, I.; Mederski, B. D.; Shadowitz, S. B.; Gold, W. L.; Hawryluck, L. A.; Rea, E.; Chenkin, J. S.; Cescon, D. W.; Poutanen, S. M.; Detsky, A. S. *J. Am. Med. Assoc.* **2003**, *289*, 2801.
- Bean, B. *Clin. Microbiol. Rev.* **1992**, *5*, 146.
- Kowdley, K. V. *J. Clin. Gastroenterol.* **2005**, *39*, S3.
- Pfeiffer, J. K.; Kirkegaard, K. *Proc. Natl. Acad. Sci. U.S.A.* **2003**, *100*, 7289.
- Pfeiffer, J. K.; Kirkegaard, K. *J. Virol.* **2005**, *79*, 2346.
- Willis, R. C.; Carson, D. A.; Seegmiller, J. E. *Proc. Natl. Acad. Sci. U.S.A.* **1978**, *75*, 3042.
- Miller, R. L.; Adamczyk, D. L.; Miller, W. H.; Koszalka, G. W.; Rideout, J. L.; Beacham, L. M.; Chao, E. Y.;

**Figure 1.** High affinity hADK substrates and inhibitors.

- Haggerty, J. J.; Krenitsky, T. A.; Elion, G. B. *J. Biol. Chem.* **1979**, *254*, 2346.
12. Long, M. C.; Parker, W. B. *Biochem. Pharmacol.* **2006**, *71*, 1671.
13. Yadav, V.; Chu, C. K.; Rais, R. H.; AlSafarjalani, O. N.; Guarcello, V.; Naguib, F. N. M.; elKouni, M. H. *J. Med. Chem.* **2004**, *47*, 1987.
14. Harki, D. A.; Graci, J. D.; Korneeva, V. S.; Ghosh, S. K. B.; Hong, Z.; Cameron, C. E.; Peterson, B. R. *Biochemistry* **2002**, *41*, 9026.
15. Zimmerman, T. P.; Deeprose, R. D. *Biochem. Pharmacol.* **1978**, *27*, 709.
16. Leyssen, P.; Balzarini, J.; De Clercq, E.; Neyts, J. *J. Virol.* **2005**, *79*, 1943.
17. Streeter, D. G.; Witkowski, J. T.; Khare, G. P.; Sidwell, R. W.; Bauer, R. J.; Robins, R. K.; Simon, L. N. *Proc. Natl. Acad. Sci. U.S.A.* **1973**, *70*, 1174.
18. Leyssen, P.; De Clercq, E.; Neyts, J. *Mol. Pharmacol.* **2006**, *69*, 1461.
19. Eriksson, B.; Helgstrand, E.; Johansson, N. G.; Larsson, A.; Misiorny, A.; Noren, J. O.; Philipson, L.; Stenberg, K.; Stening, G.; Stridh, S.; Oberg, B. *Antimicrob. Agents Chemother.* **1977**, *11*, 946.
20. Tsai, C.; Lee, P.; Stollar, V.; Li, M. *Curr. Pharm. Des.* **2006**, *12*, 1339.
21. Kentsis, A.; Topisirovic, I.; Culjkovic, B.; Shao, L.; Borden, K. L. B. *Proc. Natl. Acad. Sci. U.S.A.* **2004**, *101*, 18105.
22. Scheidel, L. M.; Stollar, V. *Virology* **1991**, *181*, 490.
23. Scheidel, L. M.; Durbin, R. K.; Stollar, V. *Virology* **1987**, *158*, 1.
24. Tam, R. C.; Pai, B.; Bard, J.; Lim, C.; Averett, D. R.; Phan, U. T.; Milovanovic, T. *J. Hepatol.* **1999**, *30*, 376.
25. Dusheiko, G.; Main, J.; Thomas, H.; Reichard, O.; Lee, C.; Dhillon, A.; Rassam, S.; Fryden, A.; Reesink, H.; Bassendine, M.; Norkrans, G.; Cuypers, T.; Lelie, N.; Telfer, P.; Watson, J.; Weegink, C.; Silikens, P.; Weiland, O. *J. Hepatol.* **1996**, *25*, 591.
26. Severson, W. E.; Schmaljohn, C. S.; Javadian, A.; Jonsson, C. B. *J. Virol.* **2003**, *77*, 481.
27. De Clercq, E. *Antiviral Res.* **2005**, *67*, 56.
28. De Clercq, E. *Curr. Opin. Microbiol.* **2005**, *8*, 552.
29. Witkowski, J. T.; Robins, R. K. *J. Org. Chem.* **1970**, *35*, 2635.
30. Gabrielsen, B.; Phelan, M. J.; Barthel-Rosa, L.; See, C.; Huggins, J. W.; Kefauver, D. F.; Monath, T. P.; Ussery, M. A.; Chmurny, G. N., et al. *J. Med. Chem.* **1992**, *35*, 3231.
31. Szychala, J.; Datta, N. S.; Takabayashi, K.; Datta, M.; Fox, I. H.; Gribbin, T.; Mitchell, B. S. *Proc. Natl. Acad. Sci. U.S.A.* **1996**, *93*, 1232.
32. Miles, D. W.; Robins, R. K. *J. Phys. Chem.* **1983**, *87*, 2444.
33. Dea, P.; Schweizer, M. P.; Kreishmans, G. P. *Biochemistry* **1974**, *13*, 1862.
34. McClure, K. F.; Abramov, Y. A.; Laird, E. R.; Barberia, J. T.; Cai, W.; Carty, T. J.; Cortina, S. R.; Danley, D. E.; Dipesa, A. J.; Donahue, K. M.; Dombroski, M. A.; Elliott, N. C.; Gabel, C. A.; Han, S.; Hynes, T. R.; LeMotte, P. K.; Mansour, M. N.; Marr, E. S.; Letavic, M. A.; Pandit, J.; Ripin, D. B.; Sweeney, F. J.; Tan, D.; Tao, Y. *J. Med. Chem.* **2005**, *48*, 5728.
35. Allen, F. H.; Baalham, C. A.; Lommerse, J. P. M.; Raithby, P. R.; Sparr, E. *Acta Cryst.* **1997**, *B53*, 1017.
36. Too, K.; Brown, D. M.; Holliger, P.; Loakes, D. *Collect. Czech. Chem. Commun.* **2006**, *71*, 899.
37. Mathews, I. I.; Erion, M. D.; Ealick, S. E. *Biochemistry* **1998**, *37*, 15607.
38. Schumacher, M. A.; Scott, D. M.; Mathews, I. I.; Ealick, S. E.; Roos, D. S.; Ullman, B.; Brennan, R. G. *J. Mol. Biol.* **2000**, *298*, 875.
39. Ketone **3**: ^1H NMR (200 MHz, CD_3OD , 25 °C): δ 8.84 (s, 1H), 5.94 (d, 1H, $J = 3.30$ Hz), 4.49 (m, 1H), 4.35 (m, 1H), 4.13 (m, 1H), 3.88–3.81 (m, 1H), 3.74–3.66 (m, 1H), 2.61 (s, 3H). ^{13}C NMR (50.3 MHz, CD_3OD , 25 °C): δ 192.4, 161.4, 146.7, 94.3, 87.1, 76.7, 71.6, 62.7, 27.1. FT-IR (KBr) cm^{-1} : 3470, 3375, 1704. LCMS (APCI) m/z : Calcd for $\text{C}_9\text{H}_{14}\text{N}_3\text{O}_5$ $[\text{MH}]^+$: 244.09; found: 244.30.
40. Acetamide **8**: ^1H NMR (300 MHz, $\text{Me}_2\text{SO}-d_6$, 25 °C): δ 10.35 (br s, 1H, NH), 8.59 (s, 1H), 5.66 (d, 1H, $J = 4.11$ Hz), 5.48 (d, 1H, $J = 5.58$ Hz), 5.13 (d, 1H, $J = 5.28$ Hz), 4.85 (t, 1H, $J = 5.57$ Hz), 4.29 (m, 1H), 4.08 (m, 1H), 3.90 (m, 1H), 3.89 (1H, m), 3.63–3.55 (m, 1H), 3.51–3.42 (m, 1H), 2.02 (s, 3H). ^{13}C NMR (75.5 MHz, CD_3OD , 25 °C): δ 171.4, 158.1, 144.9, 93.6, 87.3, 76.4, 71.9, 63.2, 23.5. FT-IR (KBr) cm^{-1} : 3415, 3112, 2533, 1696, 1543. LCMS (ESI) m/z : Calcd for $\text{C}_9\text{H}_{14}\text{N}_3\text{O}_5\text{-Na}$ $[\text{MNa}]^+$: 281.09; found: 281.05.